NCAR-TN-7

An Airplane-Mounted System for Sensing and Recording Radio Noise in Clouds

J. Doyne Sartor
Paul A. Eden

March 1966

NATIONAL CENTER FOR ATMOSPHERIC RESEARCH
Boulder, Colorado

PREFACE

The purpose of this document is to record an instrumental development which solved certain problems in field research for NCAR staff scientists, and which promises to have some wider application beyond the particular field problems which prompted the design.

CONTENTS

FIGURES

I. INTRODUCTION

The instrumentation and procedures described in this report were designed to detect and record radio noise from clouds during a field study in Key West, Florida, in the summer of 1964. Previous investigations had led us to believe that radio emissions are produced by small, growing cumulus clouds, which had not previously been considered large enough to be electrically active. Such emissions would indicate some sort of electrification process within the cloud.

We intended ultimately to use these radio emissions from clouds to determine indirectly the state of growth of the cloud and the state of growth of electrification within the cloud. It was important to try to fly the aircraft in such a way that we would be able to identify when the cloud passed through the level of the 0°C isotherm, and therefore would be in danger of having ice crystals within it. We wanted to avoid clouds with ice crystals, to simplify an already extremely complex and not very well understood phenomenon. Key West, Florida, was chosen as the site of the field study because of the regular presence of clouds that extend through considerable depth of the atmosphere before they reach the 0° isotherm.

Section II describes the receivers, sensors, and recording system. Section III outlines the flight procedures followed. Section IV gives the calibration of the electric field probes. Appendix A includes the pattern measurements of the receiver antennas mounted in the aircraft and the sensitivities of the overall system, provided under contract by the Colorado Research Corporation. Appendix B gives the schematics for the receiving and recording system (Figs. 13 through 23).

II. RECEIVING AND RECORDING SYSTEM

RADIO RECEIVERS

The radio receiving system consisted of six receivers, transistorized to provide low power consumption, high reliability, and low weight. weight. One of these, a 7.35 kc tuned RF sferics receiver with ~60 db gain, was sufficiently sensitive to record lightning throughout and beyond the area being flown. It was included to supply the University of Wisconsin sferics program with useful data from these flights. The others recorded noise in approximately octave steps at 30.0, 50.5, 144.05, 220.5, and 550.1 Mc. All six receivers were narrow-band (10 kc) to avoid interference.

The four receivers from 50 through 550 Mc each consisted of two sections: IF amplifiers and converters. Any converter could be patched into any amplifier. The 30 Mc receiver did not have a converter operating in front of it, as 30 Mc is approximately the normal IF used on all the receivers. (The actual first IF was 28.7 Mc, the second was 10.7 Mc, and the third 455 kc.)

The 30 Mc section was a double conversion receiver with a CW minimum discernible signal of .12 microvolt. The complete 30 Mc receiver is shown in Fig. 20, where it is labelled "IF module." (The system as actually constructed differed in that the input tank was tuned to 30 Mc, and the first oscillator crystal was 19.3 Mc.)

The 50 through 550 Mc converters were similar except for the number of multiplier stages. The signal from the antenna was amplified in the two RF stages (~30 db gain), and was then fed into the mixer along with the local oscillator injection signal. The resulting difference signal output was fed to the IF amplifier. After the signals were detected in the receivers, they were applied to the galvanometer recording oscillographs (see Data Recording System, p. 4).

The receivers operated from a 12-volt regulated source, derived from the 28-volt aircraft power through the appropriate regulators. The 12-volt source also supplied much of the other transistorized equipment used in the flight experiments. The DC power supply from the converters was fed through the coaxial cable along with the converter output. The RF and DC were isolated by the proper filters.

ELECTROMETERS

Electric field components were measured by probes mounted on the top and the bottom of the airplane (vertical field) and nose and tail (horizontal field). The probes were aerodynamically designed to keep moisture away from the probe insulator, which was a Teflon insert inside the aluminum body. The sensor itself was a stainless steel rod approximately 8 in. long with a 500 microcurie radioactive source mounted at its tip. This radioactive tip lowered the apparent atmospheric impedance until it matched the input of the amplifier and so could be measured. The resulting voltage on the probes was brought into the plane through Teflon coaxial cable, then applied to balanced differential amplifiers, one for horizontal and one for vertical. The amplifier input impedance was approximately 2.5×10^{11} ohms. This resistance appeared in shunt with the probes, but was high enough compared to the output impedance of the probes -- approximately 1×10^{10} ohms -- that it was expected to have little loading effect on the probe. The output of the differential amplifiers was then applied to two channels on the recording oscillographs for a permanent record of horizontal and vertical electric field components.

OUTSIDE AIR TEMPERATURE

Outside air temperature was measured by a vortex thermometer (Meteorological Research, Inc., Model 803) mounted under the wing of the aircraft. In this instrument a thermistor bead mounted in a vortex tube is wired so that the bead becomes one leg of a DC bridge. As the thermistor changes resistance with temperature, the output of the bridge also changes. The lead comes into an operational amplifier, located in the equipment racks inside the aircraft. The amplifier output drives both a meter on the control box and also the oscillographs which make a continuous record of outside air temperature. The temperature-instrument output calibration was furnished by the manufacturer.

The oscilloscope input came from the wideband IF amplifier, which could be patched into any of the individual receivers. When turned on, the scope camera ran for 5 sec out of each minute. The logic and amplifiers which ran the camera were located in the camera programmer. The programming and sequencing system performed well, but a malfunction of the camera-scope photography was discovered too late to be corrected in the field.

The 1-sec pulses also activated two time-lapse cameras. One was located in the front of the aircraft, aimed forward to photograph the cloud under study on an approach flight. The other was on the left side of the aircraft, to photograph the cloud we were working while circling either close in or at a distance. These cameras were turned on and off by a switch located on the scope and camera programmer, and they were set to operate at 1 frame/sec while the camera programmer provided the sequencing impulses for the scope photography. The scope was set for continuous operation at zero sweep speed, with horizontal definition and separation of vertical scope deflections provided by the movement of the film in the camera.

COMMUNICATIONS AND VOICE RECORDING SYSTEM

The NCAR Aviation Facility provided a communication system consisting of three Aerotron air-to-ground transceivers: one in the aircraft, one in our office at the Casa Roma Motel, and one at the radar site. In the aircraft, four plug positions were located in the cabin walls and one each at the pilot and copilot positions. Each outlet could switch to interphone, or to interphone plus air-to-ground. On our flights we used the air-to-ground positions to include the people on the ground in our conversations. A voice-operated Uher tape recorder in the aircraft recorded all conversations on this communication line during the flights.

The signal from the airplane was received at the Casa Roma where it was again recorded on a Uher tape recorder. This ground-based recording eliminated the aircraft background noise and made the playback much easier to understand.

RADAR

A surplus M-33 tracking radar was set up at the northeast end of the runway at Key West International Airport. The M-33 consisted of an S-band acquisition radar, and an X-band tracking radar, with an analog computer which operated an x-y plotting board. The radar tracked the aircraft during flight, and the track indicated on the plotting board was later used to help reconstruct the flight path in relation to the cloud position. The acquisition portion of the set was also used to determine when clouds were precipitating.

The M-33 required 400-cycle power, which was supplied by a 60-cycle to 400-cycle motor generator set, giving 400-cycle, 3-phase output at 50,000 watts. We used an aircraft/ground air conditioning unit to cool the radar and men working inside.

The air-to-ground receiver at the radar site had one headset located at the tracking radar, and another at the plotting board. Thus both operators could communicate with the aircraft and with the office, and their conversation was included in both recordings.

SPORADIC E INTERFERENCE

During the flight program we found we were receiving interference on our 50-Mc receiver from sporadic E propagation. When the interference was present we could not use data from 50 Mc and below, because the origin of the information was ambiguous. We monitored sporadic E from 30 to 55 Mc on the ground with a tuneable system consisting of a Drake Model TR-3 transceiver and a 50-Mc converter similar to the one used in the aircraft. With this system we determined periods of interference, and could eliminate contaminated data from our cloud noise studies.

FLIGHT INFORMATION

The NCAR Research Aviation Facility provided an auxiliary flight data panel with an intervalometer camera not synchronized to the scientific data-recording master timer. This panel gave information on altitude, true air speed, heading, VOR (direction from a station), DME (distance from a point), rate of climb, and included a digital scientific timer. This system was of limited value in our operation, because of malfunction and focusing problems with the camera and infrequent zeroing of the VOR. Spurious EM emission from the flight data panel interfered with the University of Wisconsin 610 Mc sferics receiver installed for Stig Rossby for planned joint flights. The joint flights were cancelled and a separate flight scheduled for Rossby for which the data from the instrumentation described in this report were not available.

INFLIGHT AIRCRAFT ANTENNA CALIBRATION FROM PELICAN SHOALS

Inflight aircraft antenna calibrations were attempted at 50 Mc and 144 Mc, using a transmitter operated by George Saum of the NCAR Field Observing Support Facility, from a small sandbar about 6 miles off the southern coast of the Keys. Although these efforts provided valuable qualitative information on the antenna patterns in the vertical, quantitative calibrations were impossible because of the lack of accurate tracking information. The radar could not pick up the aircraft at the low flight altitudes needed for calibration, and the auxiliary flight data panel information was not available as previously described.

III. FLIGHT PROCEDURES

Several flight patterns were attempted in trying to find one which would best locate the specific source of the radio signals originating from a cloud. We have termed the pattern that finally evolved "The Butterfly Pattern." In this procedure we cruised at approximately 10,000 ft until we found a suitable cloud, and then headed directly toward the visual center of this cloud. When we thought we were about to intercept the cloud we made a sharp right turn, and circled the cloud for a 90° arc, and then made another sharp turn and headed directly away from the cloud, 90° from the heading prior to the latter turn. After several miles, we made a sharp left turn and circled the cloud at a distance for a 90° arc. Upon completing the arc, we made a sharp left turn and headed back directly toward the cloud. Just before we intercepted the cloud we made another sharp right turn and circled 90°, in close.

The Butterfly pattern (Fig. 1) was formed by repeating this pattern until the cloud either died or passed through the 0°C isotherm, or until we abandoned research on that particular cloud.

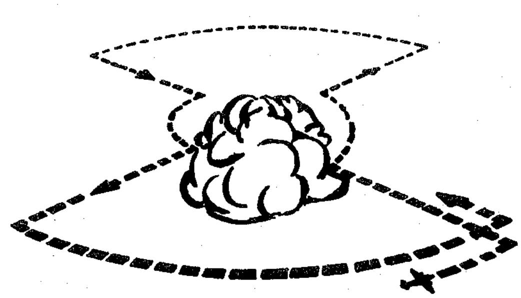

Fig. 1 - The butterfly pattern

IV. CALIBRATION OF ELECTRIC FIELD PROBES

The electric field probes were calibrated by flying in close to a thunderstorm until the aircraft and antennas went into corona and then setting the electric field recording to show deflection in this range of field. Thus whenever we observed a significant deflection of the field, we knew that the field was of the order of magnitude associated with thunderstorms, but did not know its absolute value. The main importance of the electric field was to determine when we were about to go into corona and, for data analysis purposes, to determine when corona was present, because this was a source of spurious radio information. No temperature calibration was made, since the instrument that we used was purchased from the Meteorological Research, Inc. in Altadena, and was a vortex thermometer, supposedly self-compensating.

Appendix A

NCAR QUEEN AIR AIRCRAFT ANTENNA-RECEIVER-RECORDER CALIBRATION

George Saum, Colorado Research Corporation*

*Now with the staff of the NCAR Field Observing Support Facility

NCAR QUEEN AIR AIRCRAFT ANTENNA-RECEIVER-RECORDER CALIBRATION

This Appendix provides the necessary information to convert recorded radio noise to field strength voltages at the five measurement frequencies at which noise data were collected (30, 50, 144, 220 and 550 Mc).

TEST SET-UP FOR ANTENNA PATTERN MEASUREMENTS

To obtain the horizontal plane pattern for each frequency the following procedure was carried out:

A location free of nearby objects was selected and a 100-ft radius circle was surveyed and divided into segments of 10°. A known input RF voltage was impressed on a vertically oriented half-wave transmitting dipole, and the field strength at the circle's center was measured. The measuring equipment was an Empire Device noise and field intensity meter NF105 and appropriate antenna, elevated to the same height as the transmitting dipole. To check for transmitter pattern symmetry, several azimuth positions were tried at each of three frequencies (144, 220 and 550 Mc). The measured field thus became a reference for subsequent pattern determinations.

At 30 and 50 Mc a slightly different procedure was followed. A standard loop, carrying a known RF current, was used as a transmitting source. The RF field maximum, E, existing at the circle center was calculated, using the following equation:

$$E = \frac{120\pi^2 I}{2\lambda} A \quad \text{volts/meter}$$

where I = loop current = 9×10^{-3} amps

r = distance = 30.48 meters

λ = wavelength (meters)

A = area of loop = $\frac{\pi(\text{Dia})^2}{4}$ (meters^2) = 5.06×10^{-2} meters

Thus at 30 Mc the field, E, is 177 microvolts/meter, and at 50 Mc it is 492 microvolts/meter. At the other frequencies, the field is:

144 Mc	75 db above 1 microvolt/meter
220 Mc	75 db above 1 microvolt/meter
550 Mc	70.5 db above 1 microvolt/meter

With these standard fields established, the aircraft was moved into position with the desired antenna on the aircraft centered at the circle's center. All receiver cables were installed and terminated in 50 ohms and the NF105 was connected to the desired antenna. The transmitting antenna was moved, in turn, to each of the thirty-six 10° positions. At each position the terminal voltage was measured using the NF105. The resulting tabulation of voltages provides sufficient information to construct a polar "antenna factor" plot. The antenna factor is the summation of the following parts:

1. Effective height of antenna (meters)
2. All cable losses (db)
3. Mismatch between cable and antenna (db)
4. Loading due to other receiver cables and terminations (db)

The antenna factor permits a conversion from field strength to receiver input voltage.

CALIBRATION OF RECEIVER-RECORDERS

Each receiver and recorder channel was adjusted so that a 1-in. deflection was obtained at an RF input voltage just below receiver saturation. This voltage, together with the minimum discernible RF input voltage, was measured and recorded at each frequency.

SYSTEM TRANSFER CHARACTERISTIC

By definition, the system transfer characteristic is the relation between field strength (volts/meter) and recorder deflection for each frequency, at a 0° (nose-on) azimuth position. It is obtained by combining the antenna factor with the receiver-recorder calibration.

For an azimuth position other than 0°, a correction factor must be applied to the abscissa of the transfer characteristic plot. This correction factor relates the change in antenna factor due to antenna pattern changes. It is expressed in decibels and can be converted to an abscissa multiplier by using the decibel conversion chart (Fig. 2). The minimum discernible signal (MDS) is noted on each plot and is considered to be equal to 0.05 in. of recorder deflection in all cases. There may be a slight non-linearity in some channels when working on this part of the curve. It was also assumed that the receiver/recorder channels were linear between MDS and saturation.

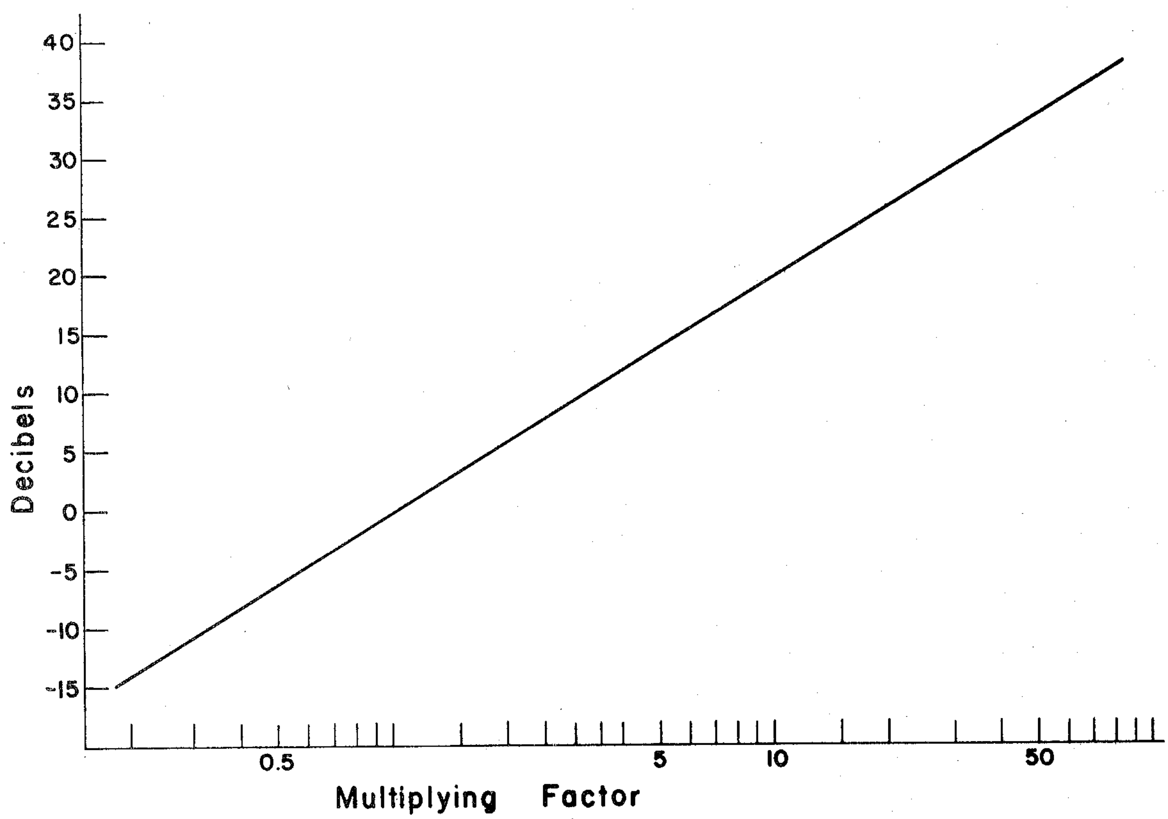

Fig. 2 - Decibel conversion chart

DISCUSSION AND ESTIMATION OF SYSTEM INACCURACY

To establish a measure of confidence in the polar plots and antenna factors, an "end-to-end" calibration run was made. This test consisted of generating a known field which should correspond to 1-in. recorder deflection, when all gains and losses in the system are present. Table 1 shows the results of this test. At all frequencies except 550 Mc the field is within 2 db of the expected value. At 550 Mc the frequency stability of the signal generator probably accounts for the large error.

Table 1 - Receiver sensitivities and recorder deflection

Frequency (Mc)	MDS (μv)	Input RF for 1-in. deflection (μv)	Input RF for complete saturation (μv)	Deflection at complete saturation (μv)	Input RF for 1-in. deflection (db/μv)	Field strength for 1-in. deflection (μv/meter)	Field strength for MDS (μv/meter) (=0.05 in.)
30	0.12	5	8.6	1.3	14	14.1	0.446
50	0.1	2.8	5.0	1.2	8.95	1.585	0.0398
144	<0.2	2.0	4.0	1.15	6.02	35.4	0.706
220	<0.2	1.9	3.5	1.2	5.56	12.6	0.398
550	<0.3	5.0	8-10	1.1	14	590	37.6

This test does not verify directly the accuracy of the antenna factors; however, a large discrepancy would remain if the antenna factors were not correct.

Another possible source of error occurs at 30 Mc where the dimension of 100 ft does not place the receiving antenna completely in the far field. At this distance an induction field component is present which is not accounted for in the calculated field. Evidently the influence of this component is small and is not a source of concern in the presence of other measurement inaccuracies.

Table 2 summarizes the receiver/recorder settings at minimum signal and saturation.

Table 2 - Summary of receiver/recorder settings at minimum signal and saturation

Frequency (Mc)	Field strength required for 1-in. deflection (db above 1 μv/meter)	Actual field for 1-in. deflection (db above 1 μv/meter)
30	23	22
50	4	5.95
144	31	32
220	22	21.5
550	55.5	49.5

This calibration has resulted in our fairly strict attention to keeping the aspect of the aircraft and antenna constant with respect to the cloud, and we evolved the butterfly pattern for this reason.

Figures 3 through 7 give antenna factor deviations from nose-on aspect, for the five receiver frequencies. Figures 8 through 12 give system transfer characteristics for the same frequencies.

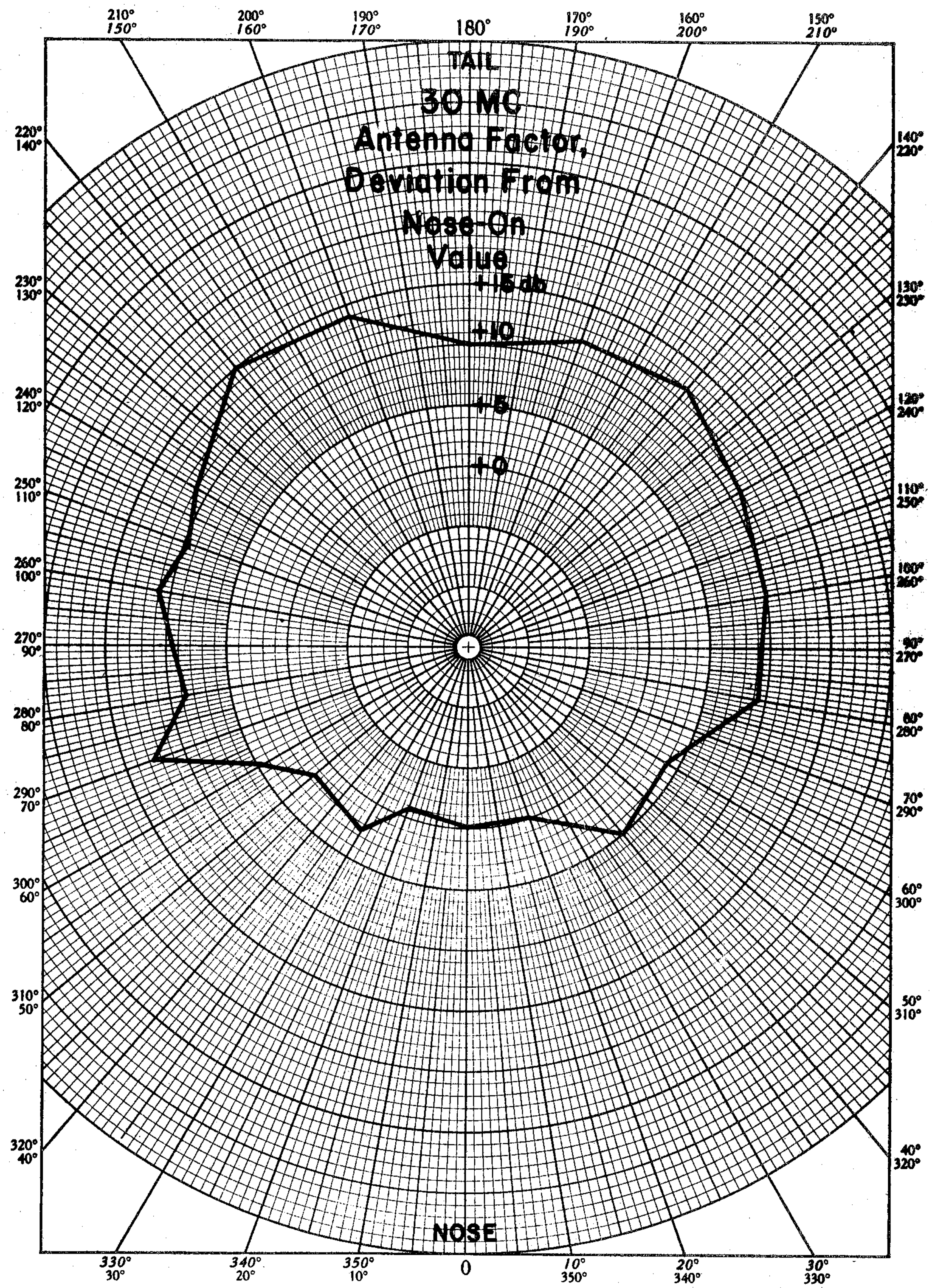

Fig. 3 - 30 Mc antenna factor deviation from nose

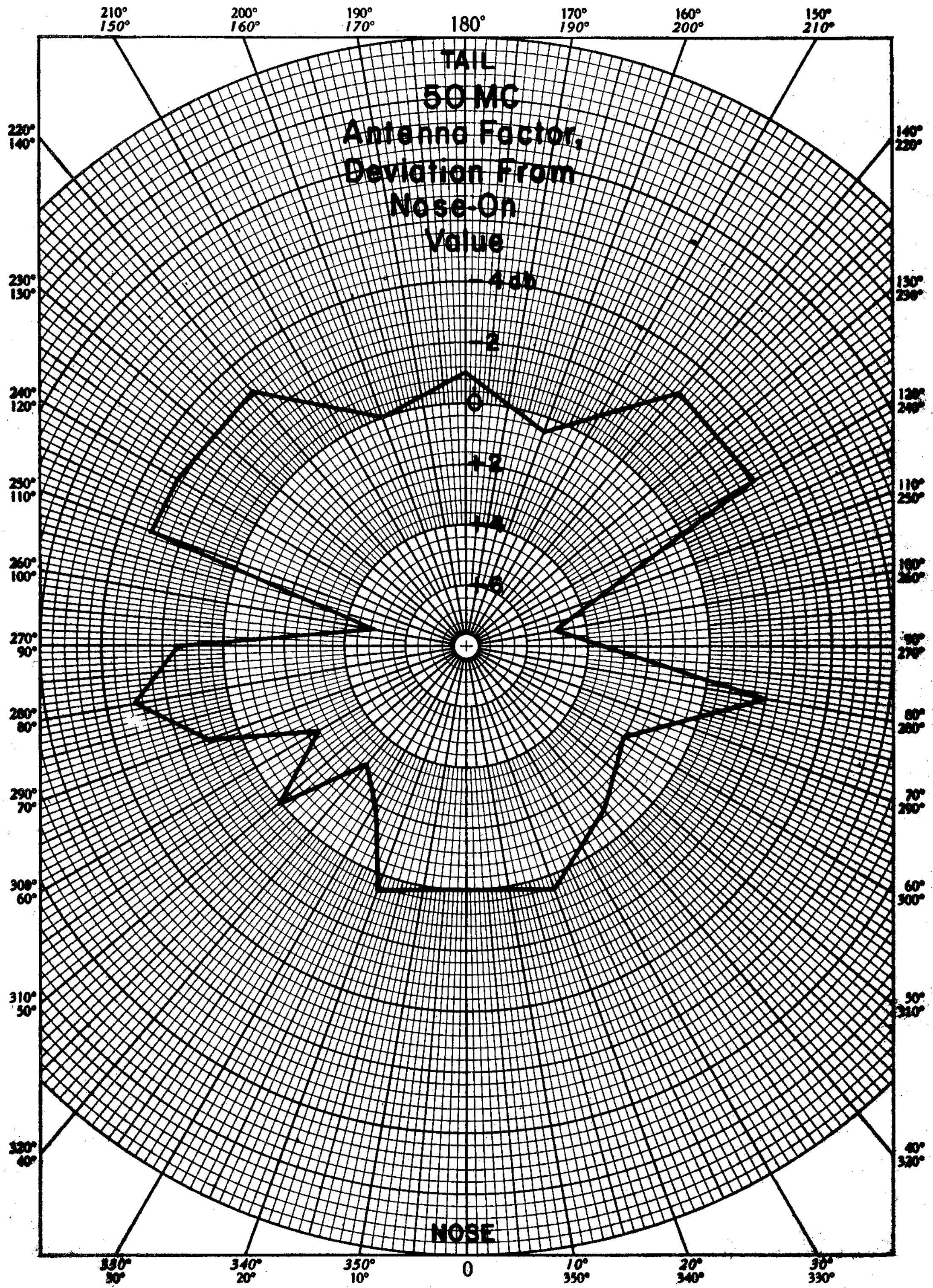

Fig. 4 - 50 Mc antenna factor deviation from nose

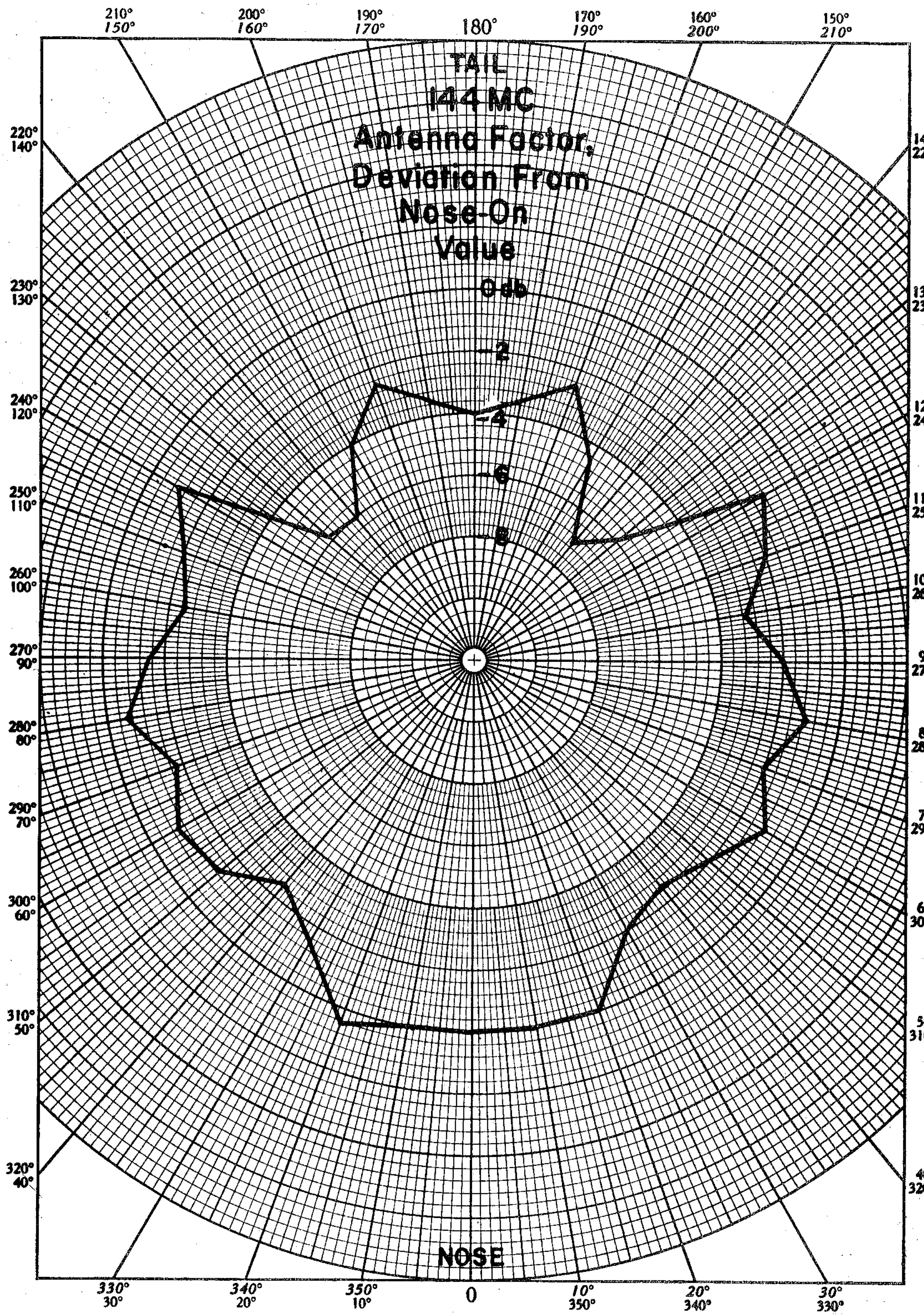

Fig. 5 - 144 Mc antenna factor deviation from nose

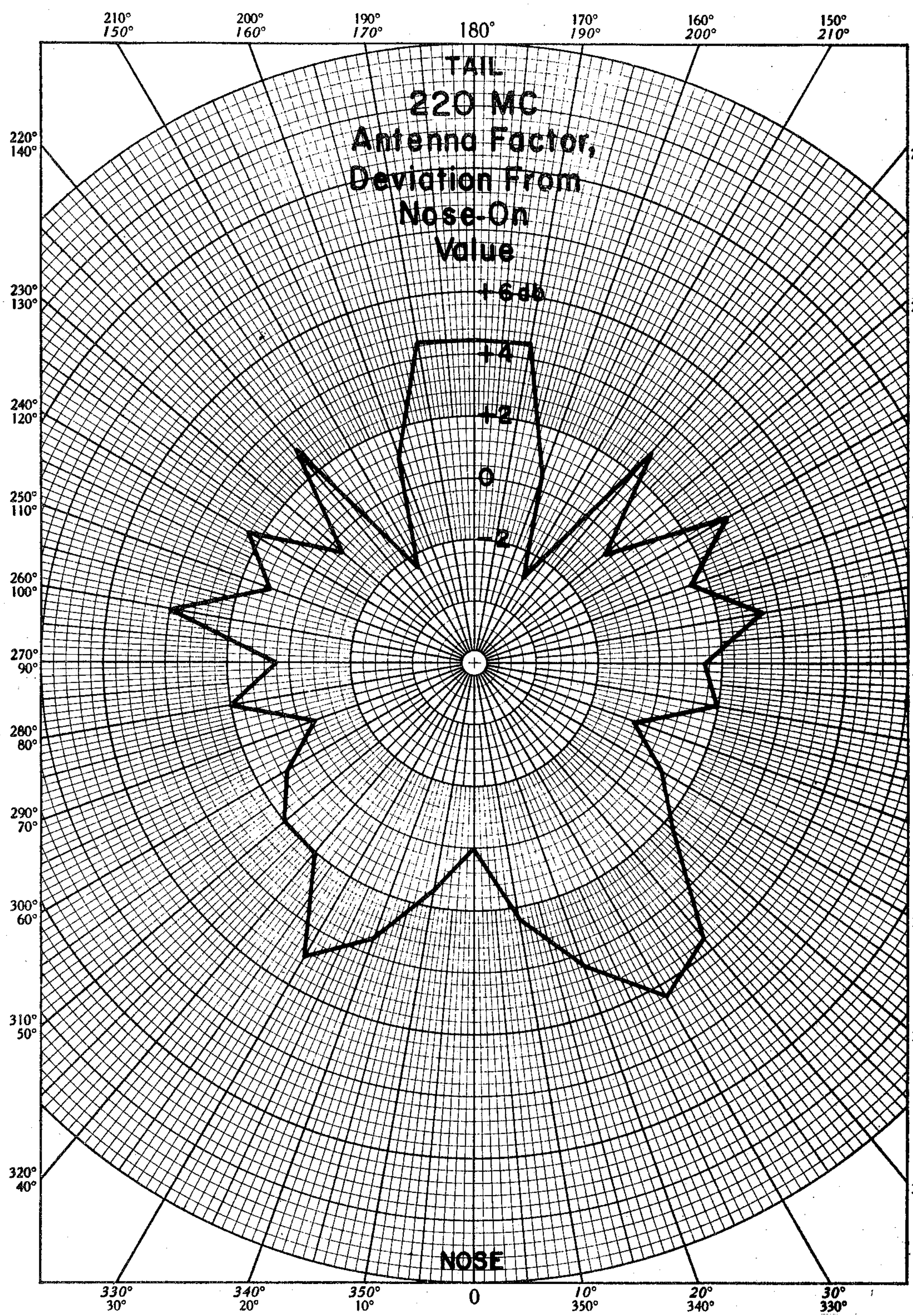

Fig. 6 - 220 Mc antenna factor deviation from nose

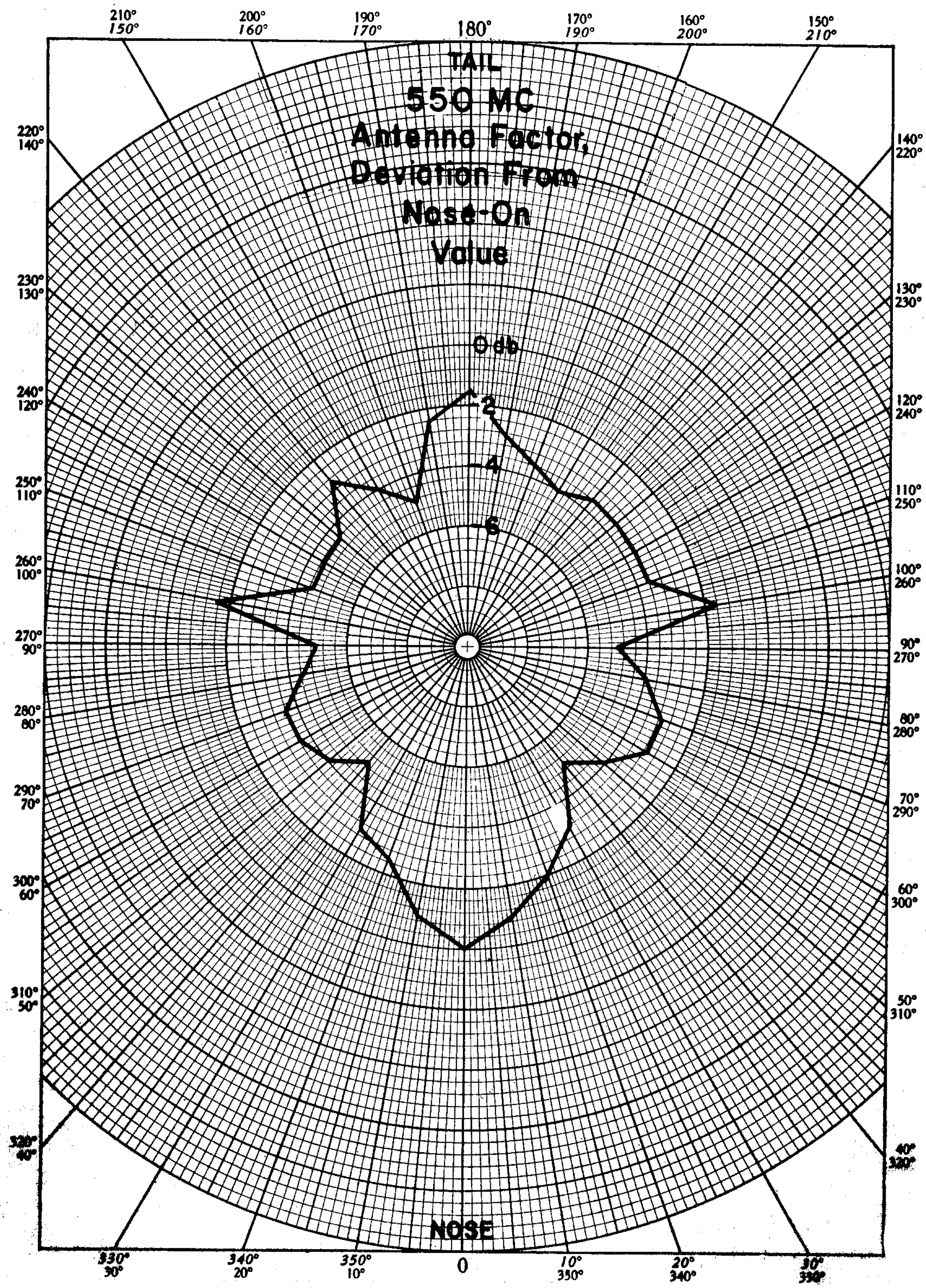

Fig. 7 - 550 Mc antenna factor deviation from nose

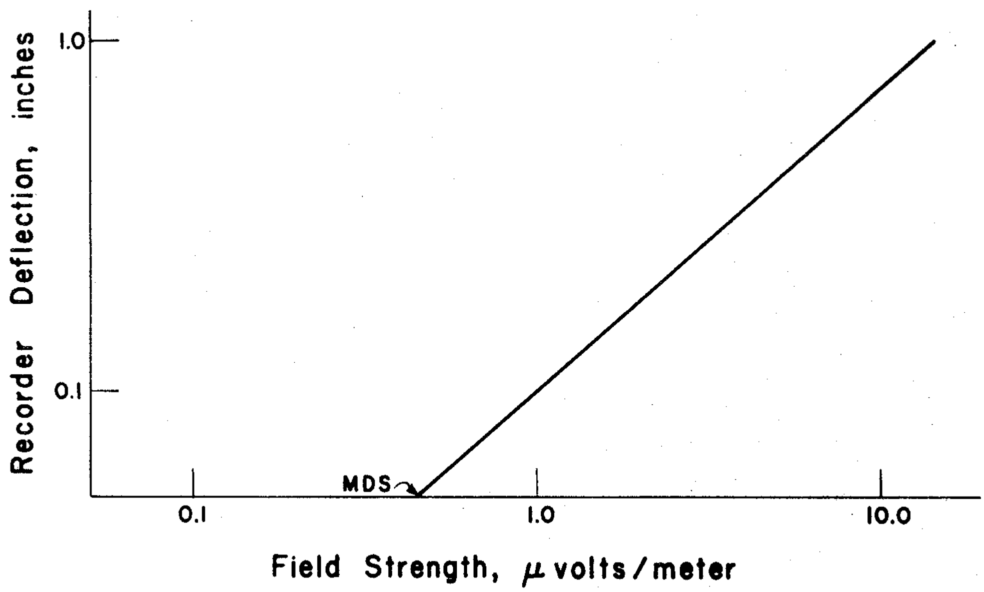

Fig. 8 - 30 Mc system transfer characteristic based on 0° azimuth

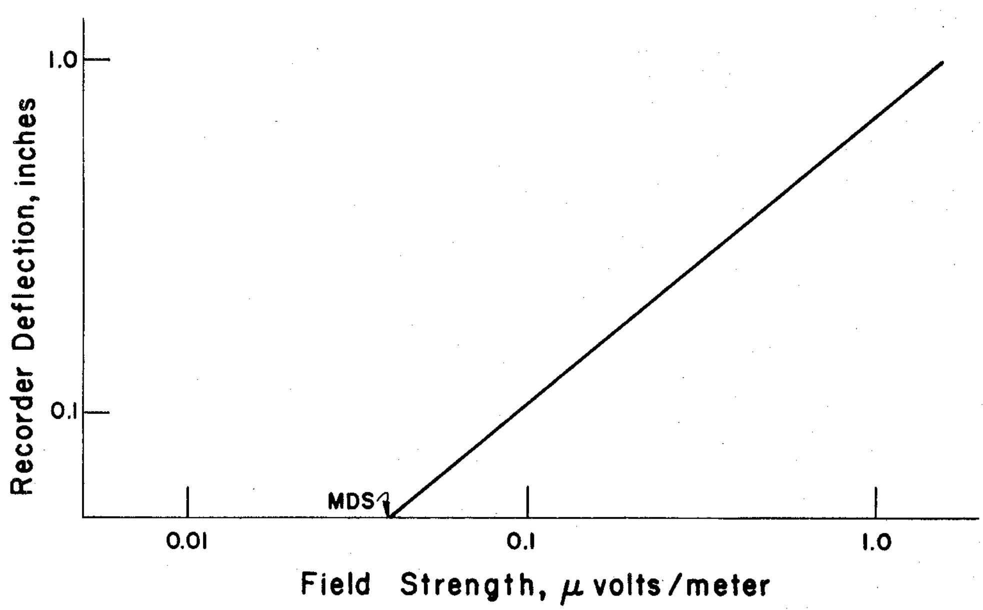

Fig. 9 - 50 Mc system transfer characteristic based on 0° azimuth

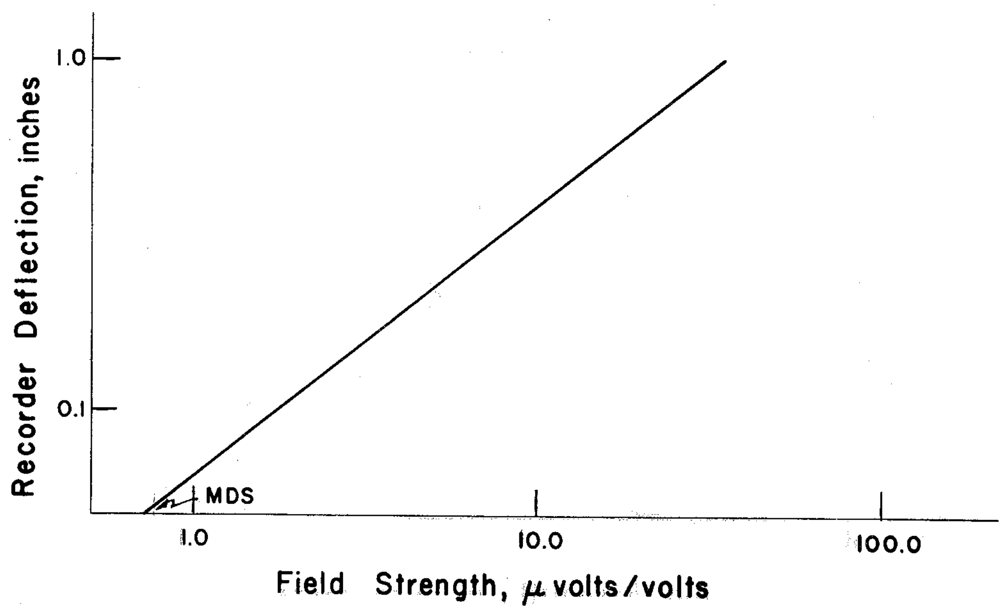

Fig. 10 - 144 Mc system transfer characteristic based on 0° azimuth

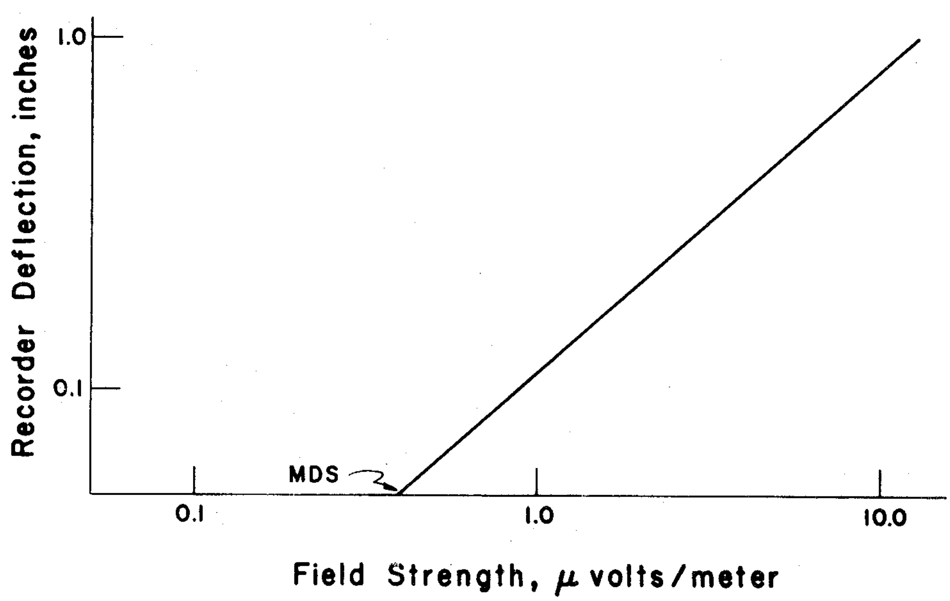

Fig. 11 - 220 Mc system transfer characteristic based on 0° azimuth

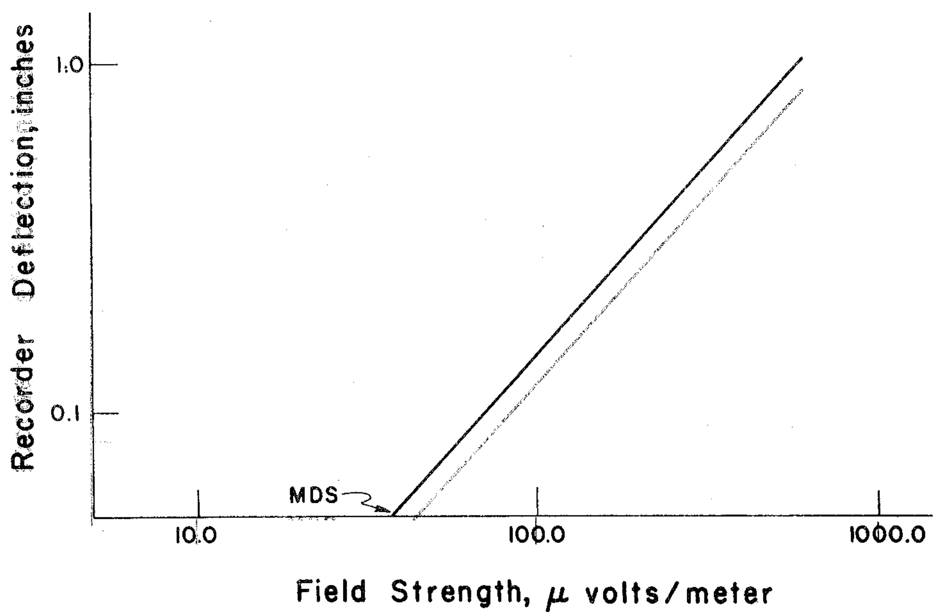

Fig. 12 - 550 Mc system transfer characteristic based on 0° azimuth

Appendix B

SCHEMATIC DIAGRAMS (Figs. 13 through 23)

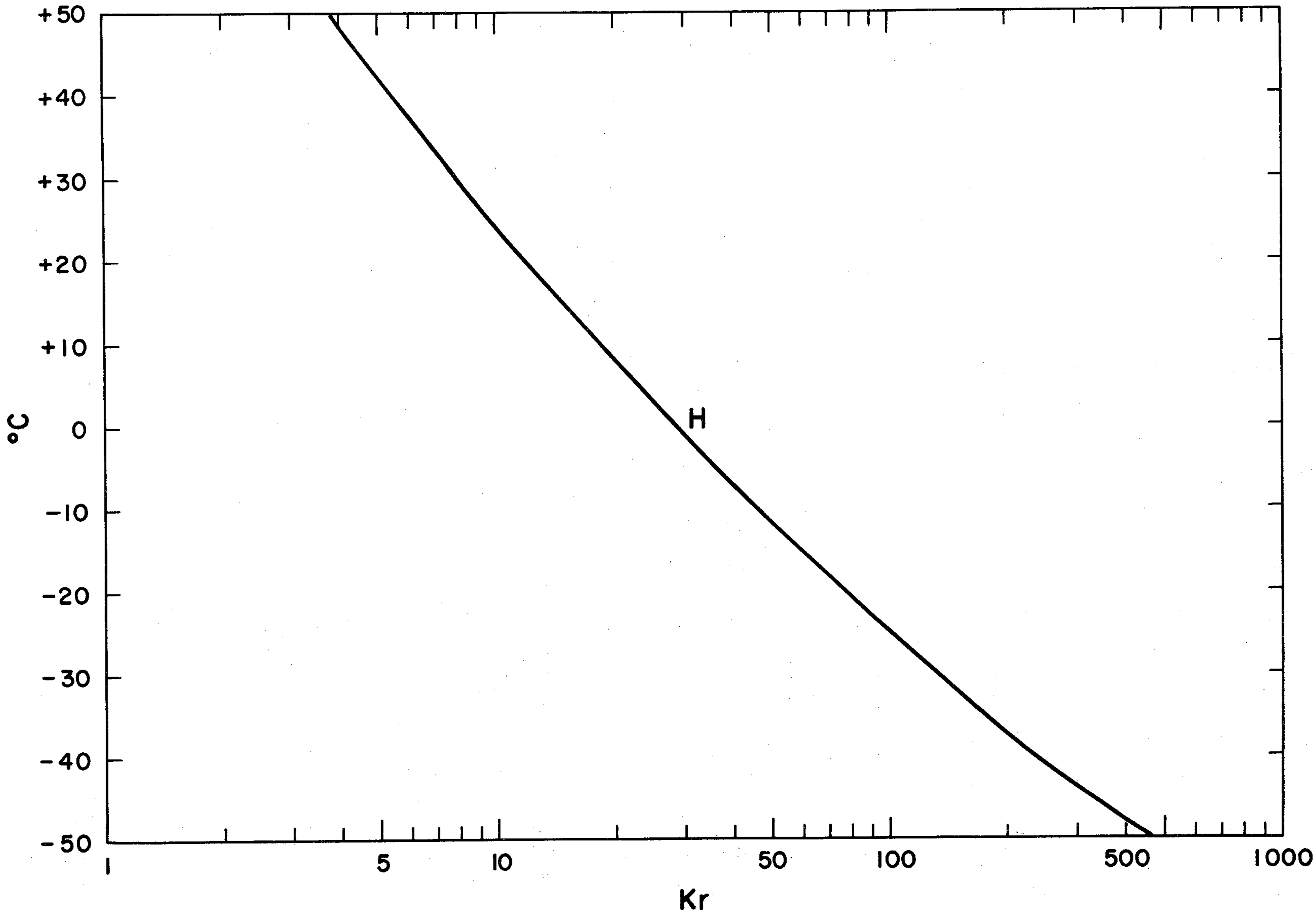

Fig. 13 - Temperature bridge curve

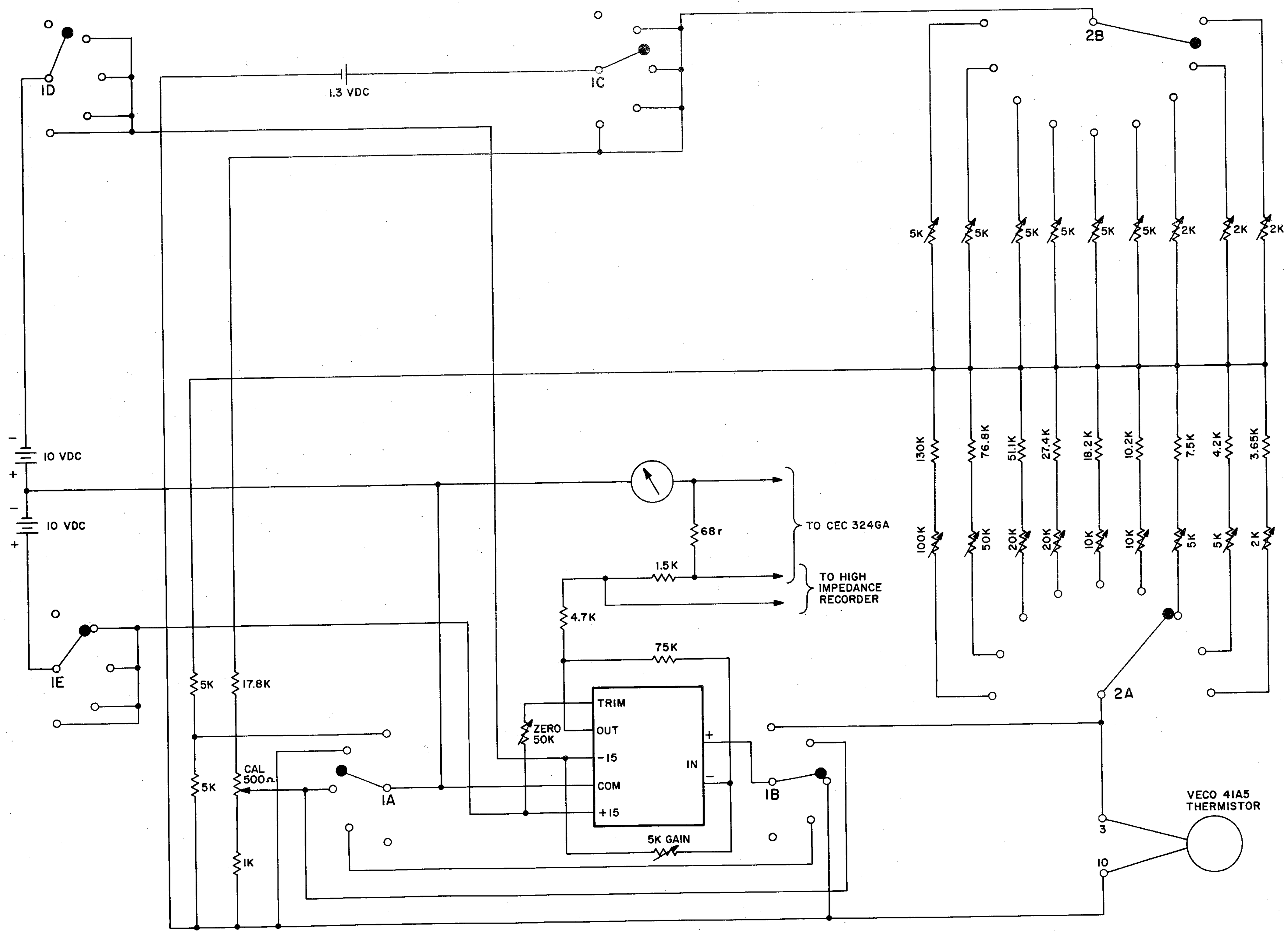

Fig. 14 - Temperature Bridge Model 803 (MRI Temperature Indicator)

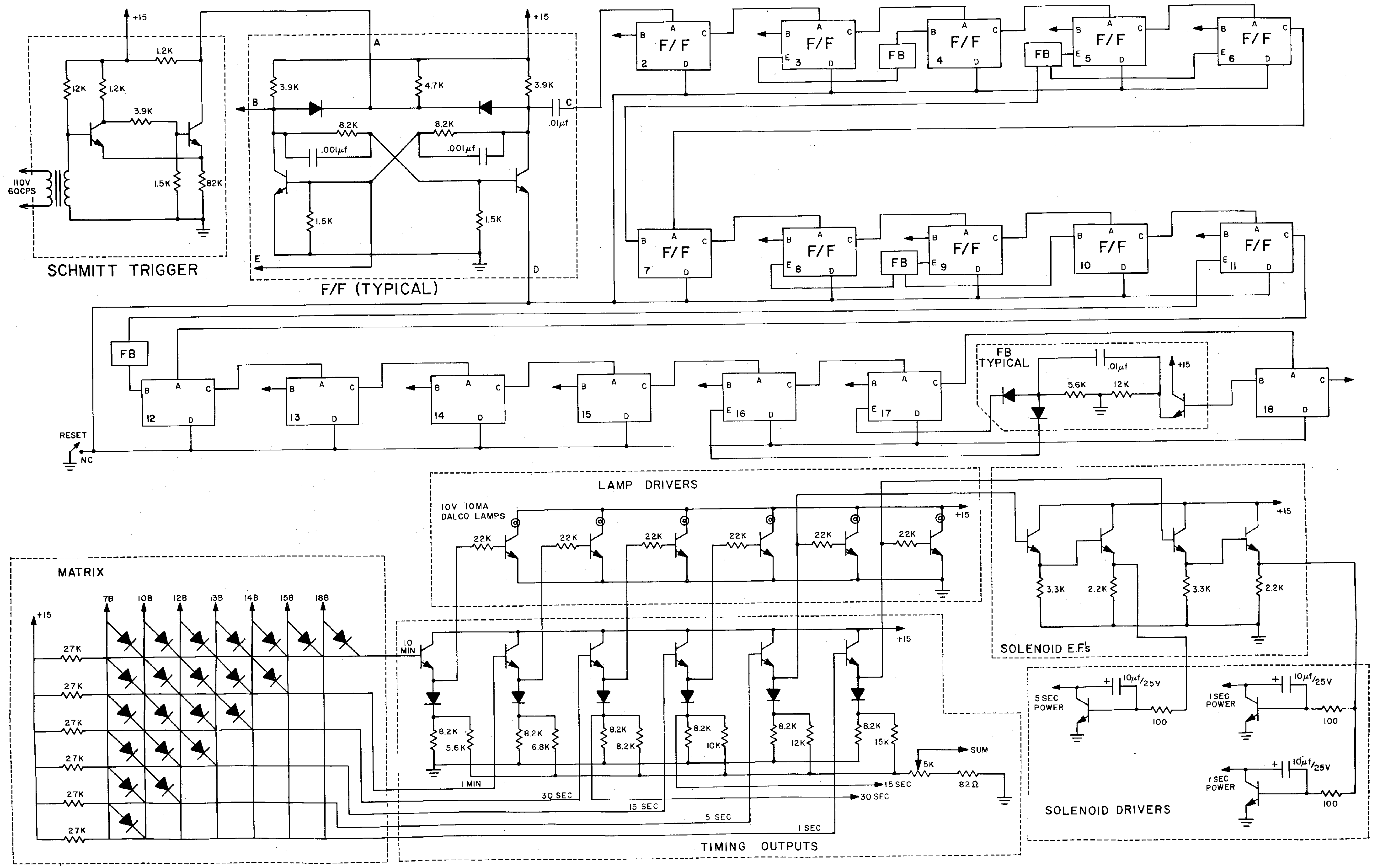

Fig. 15 - Timing generator and timer

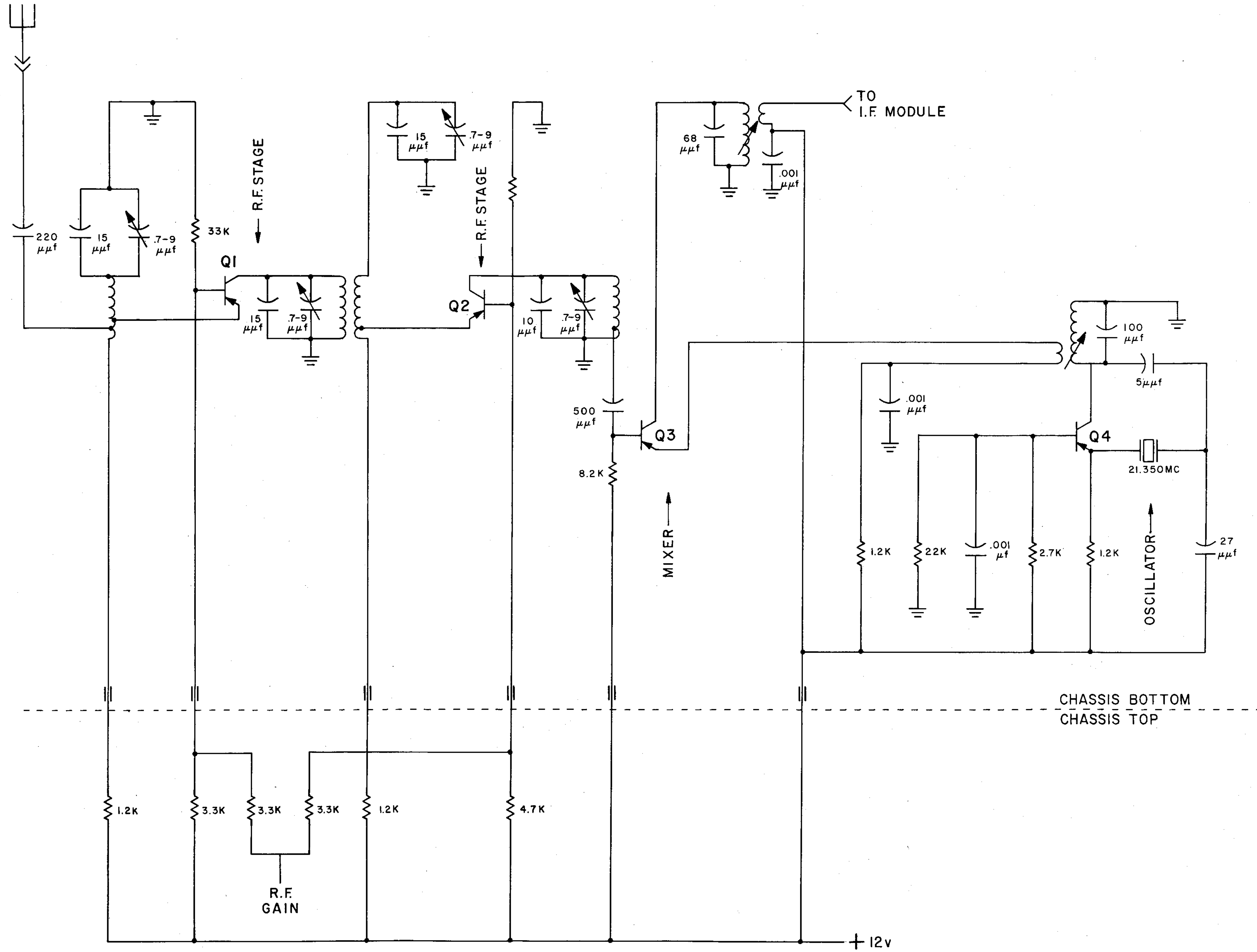

Fig. 16 - 50 Mc converter

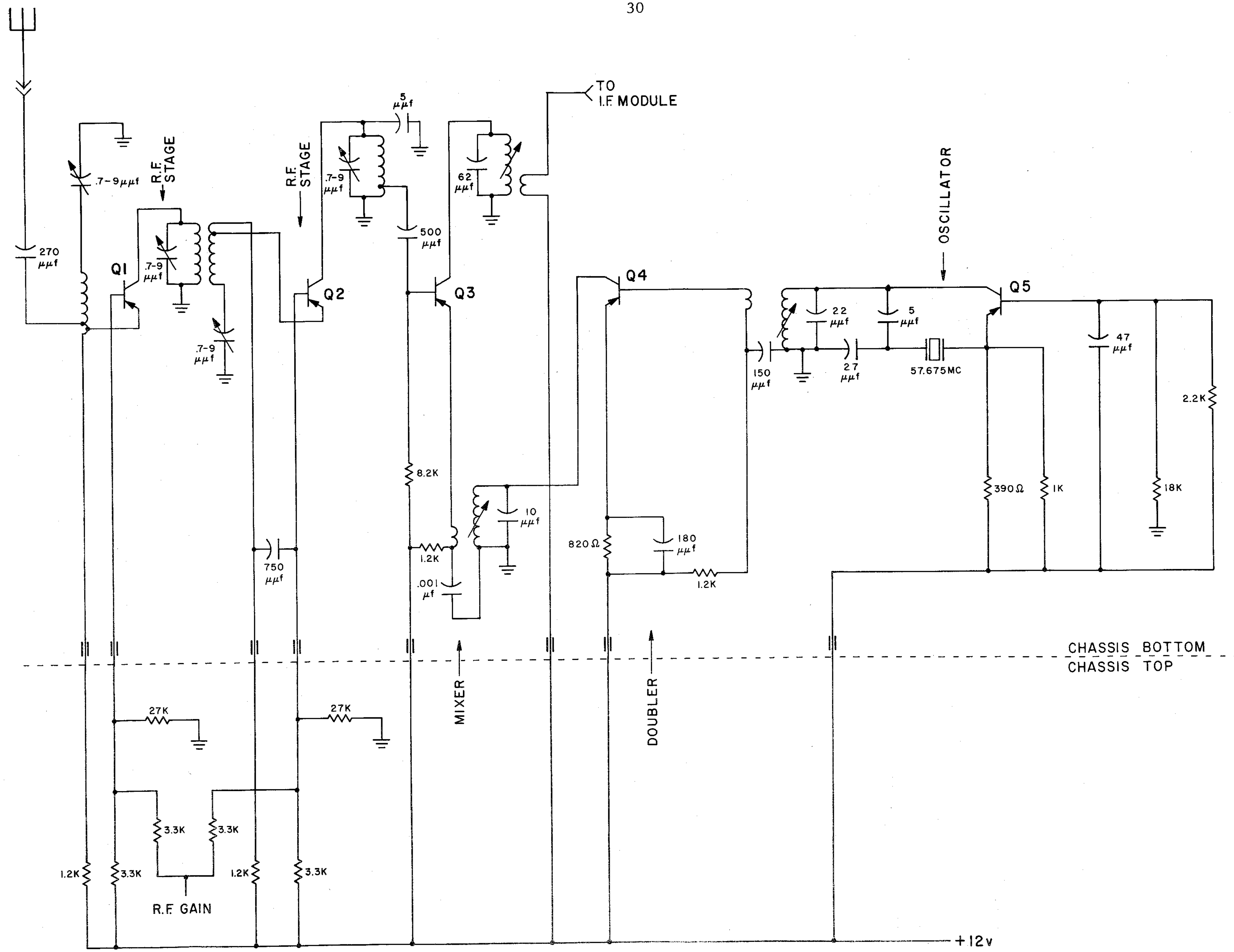

Fig. 17 - 144 Mc converter

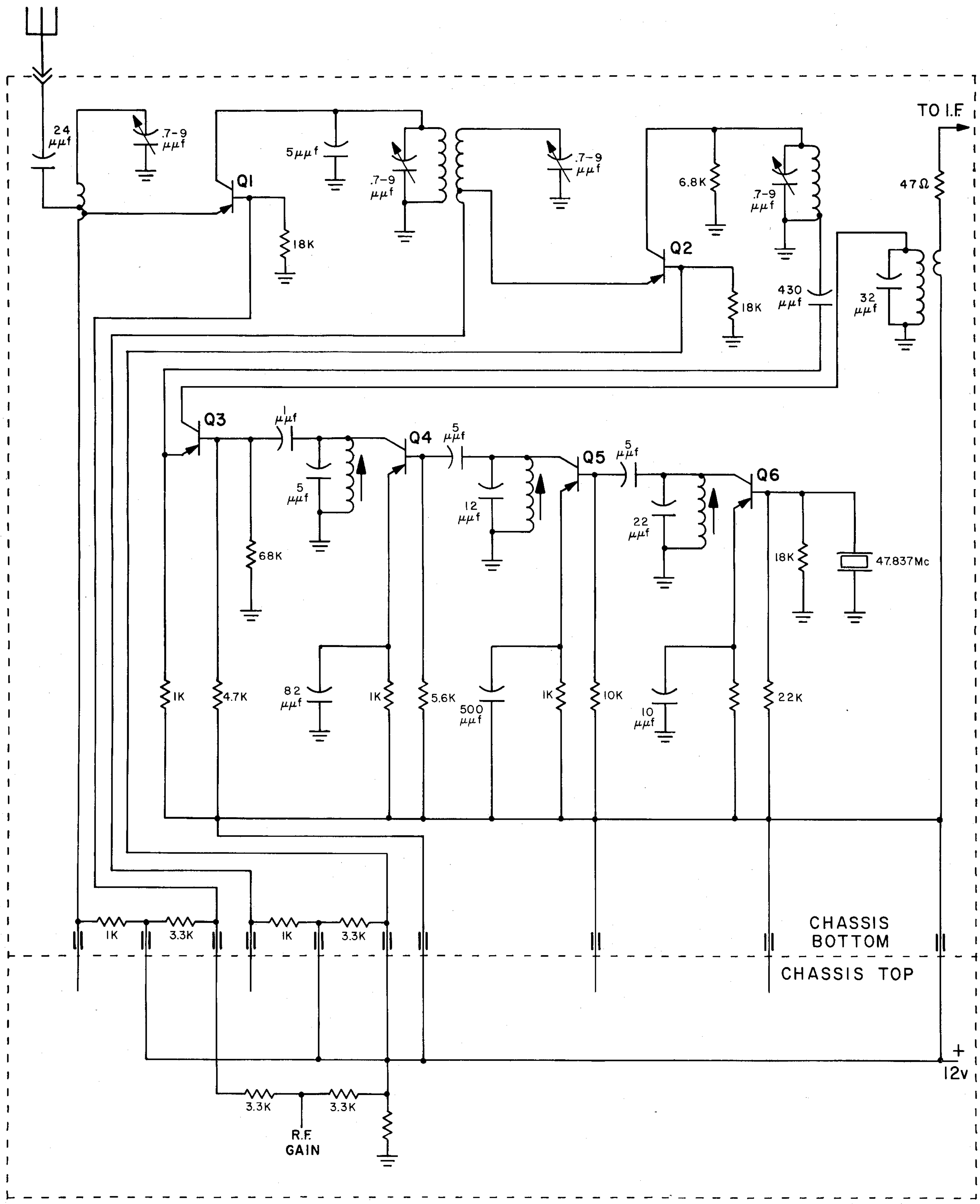

Fig. 18 - 220 Mc converter

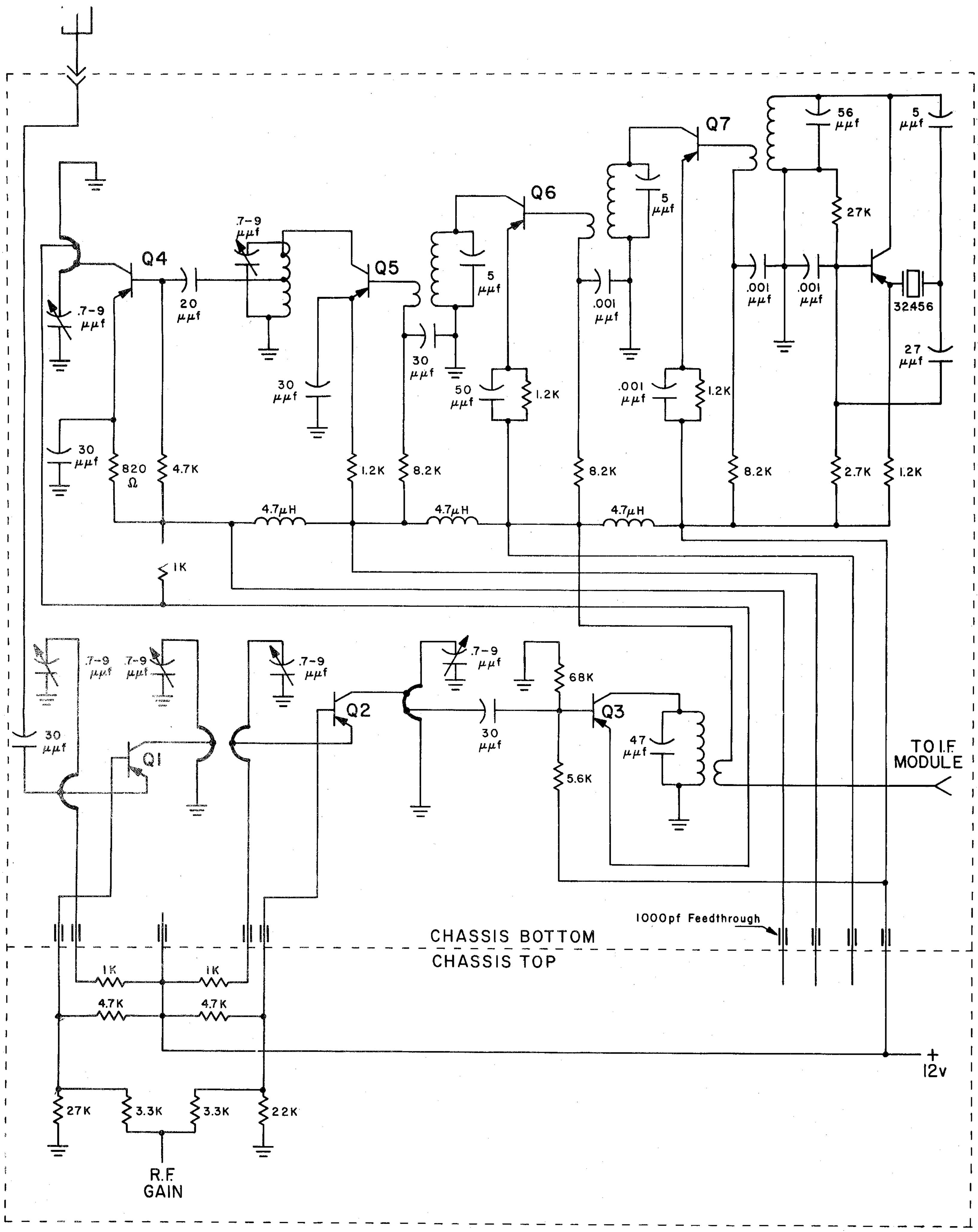

Fig. 19 - 550 Mc converter

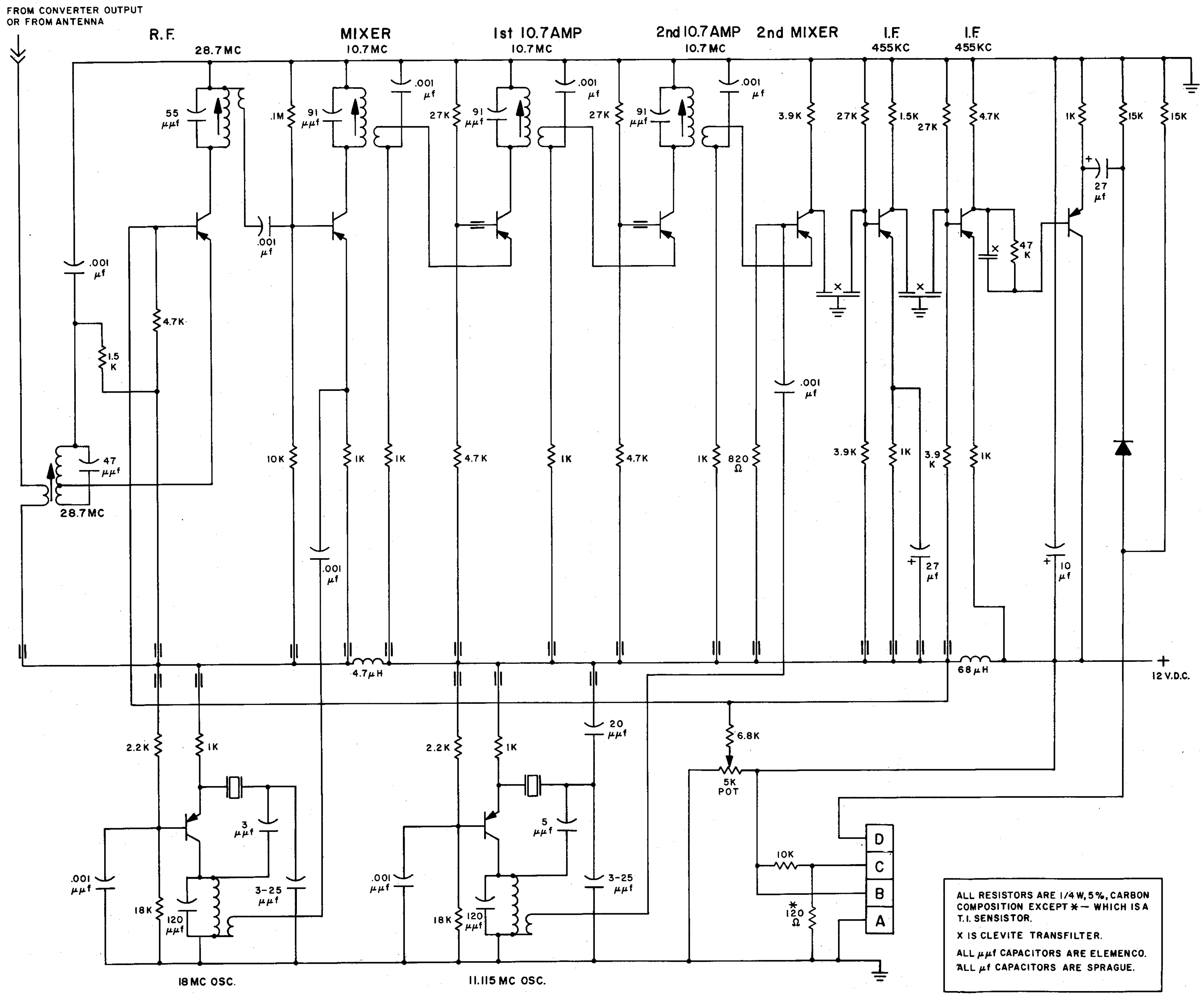

Fig. 20 - IF module

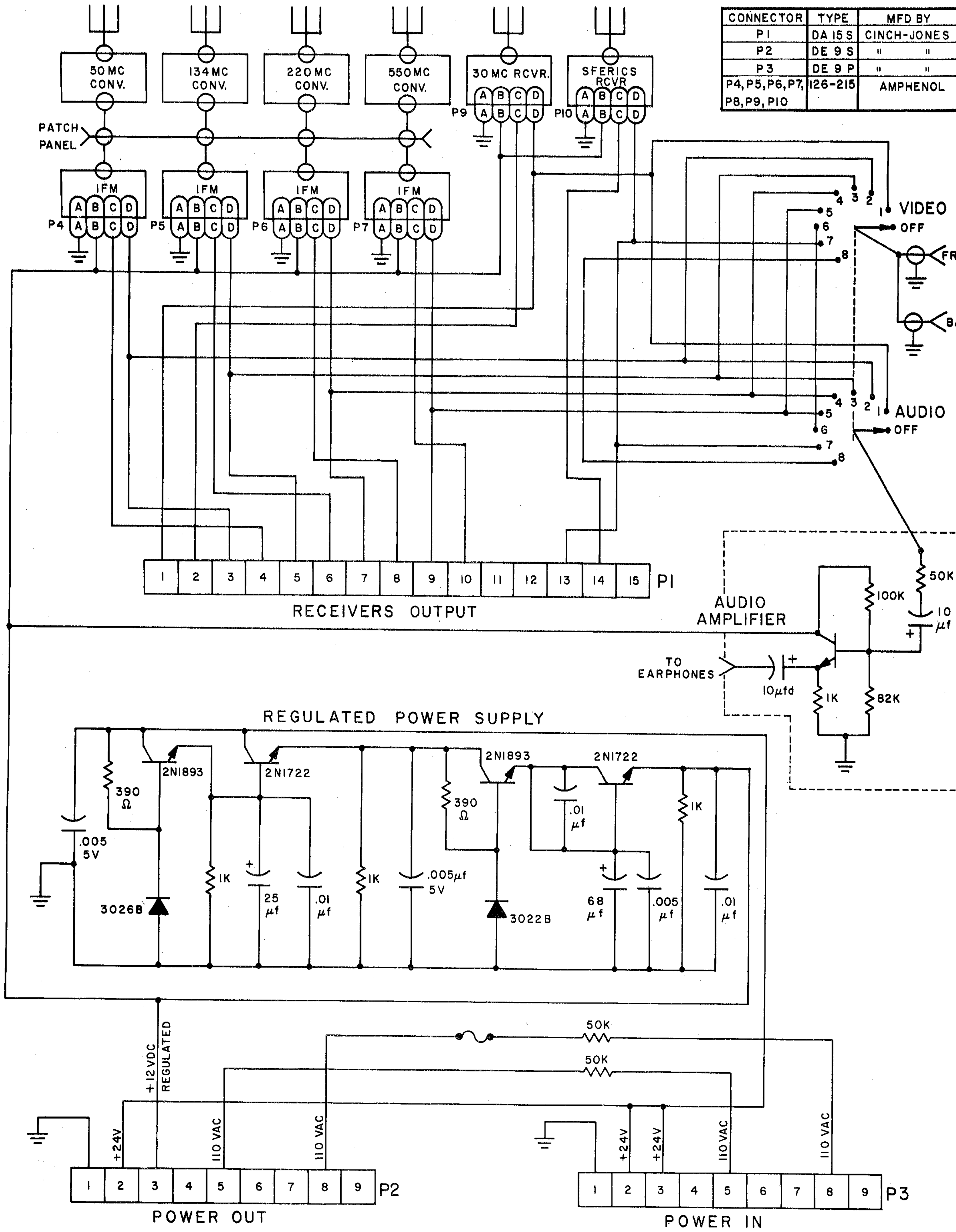

CONNECTOR	TYPE	MFD BY
P1	DA 15 S	CINCH-JONES
P2	DE 9 S	" "
P3	DE 9 P	" "
P4, P5, P6, P7, P8, P9, P10	126-215	AMPHENOL

Fig. 21 - Receiver modules and power supply

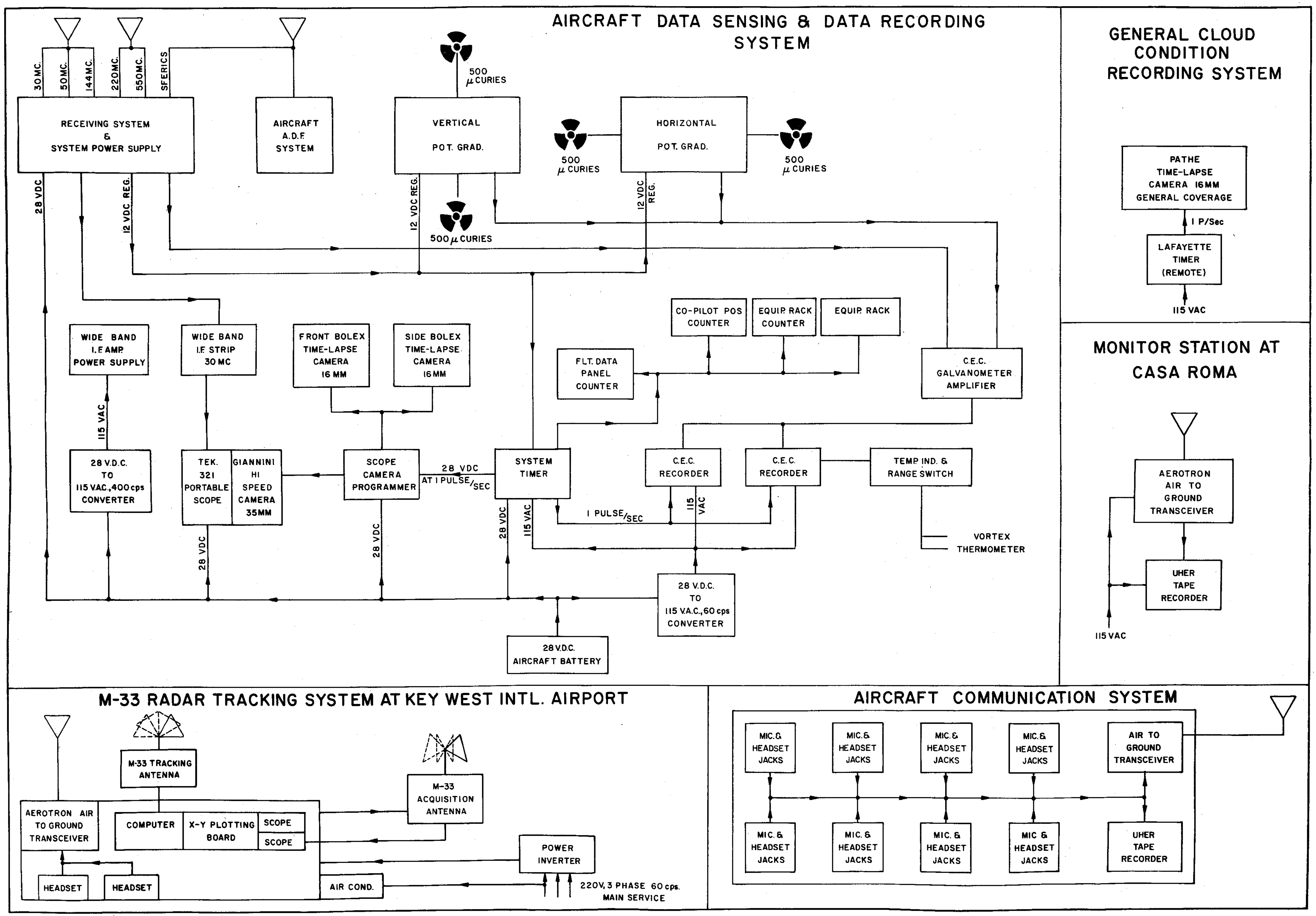

Fig. 22 - Sensing, recording and monitoring equipment

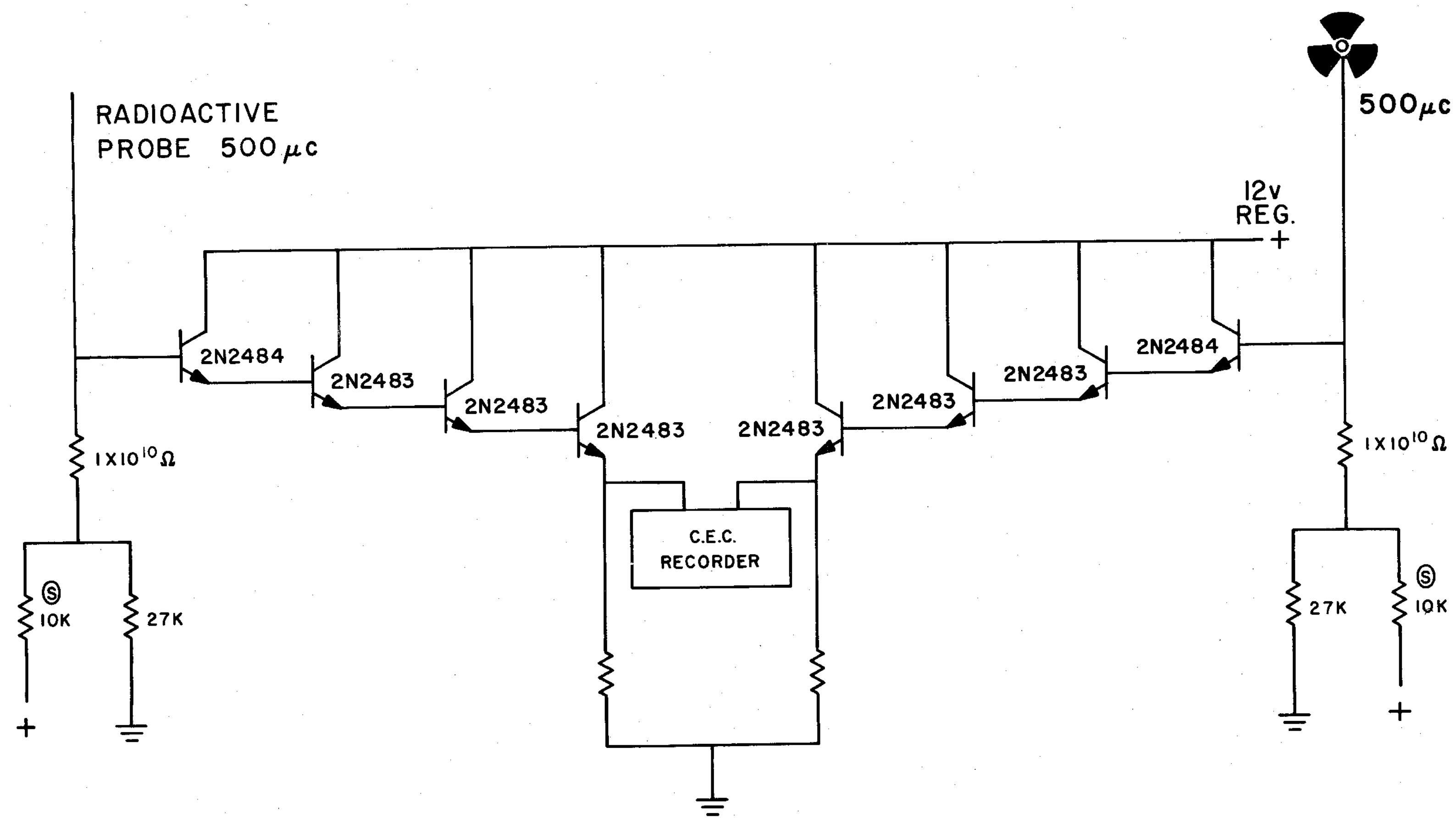

Fig. 23 - Electric field amplifier